

See discussions, stats, and author profiles for this publication at: <https://www.researchgate.net/publication/231700496>

Synthesis and Characterization of a New Series of Blue Fluorescent 2,6-Linked 9,10-Diphenylanthrylenephenylene Copolymers and Their Application for Polymer Light-Emitting Diodes

ARTICLE in MACROMOLECULES · MARCH 2010

Impact Factor: 5.8 · DOI: 10.1021/ma100195m

CITATIONS

33

READS

37

3 AUTHORS:



Hung-Yang Chen

Imperial College London

11 PUBLICATIONS 168 CITATIONS

SEE PROFILE



Chin-Ti Chen

Academia Sinica

160 PUBLICATIONS 5,470 CITATIONS

SEE PROFILE



chao-tsen Chen

National Taiwan University

71 PUBLICATIONS 2,104 CITATIONS

SEE PROFILE

Synthesis and Characterization of a New Series of Blue Fluorescent 2,6-Linked 9,10-Diphenylanthrylenephylene Copolymers and Their Application for Polymer Light-Emitting Diodes

Hung-Yang Chen,^{†,‡,§} Chin-Ti Chen,^{*,†} and Chao-Tsen Chen^{*,§}

[†]Institute of Chemistry, Academia Sinica, Taipei, Taiwan 11529, [‡]Nano Science and Technology Program, TIGP, Academia Sinica, Taipei, Taiwan 11529, and [§]Department of Chemistry, National Taiwan University, Taipei, Taiwan 10617

Received January 26, 2010; Revised Manuscript Received March 18, 2010

ABSTRACT: A series of new 9,10-diphenylanthracene-based, 2,6-linked blue-light-emitting copolymers bearing hole- or electron-transporter as well as bulky substituent were successfully synthesized. Photo-physical, thermal, electrochemical, and electroluminescence (EL) properties of these copolymers were studied and characterized. Bright and efficient blue fluorescence in the solid state was achieved by incorporating bulky substituent into the copolymer backbone. Both hole- and electron-transport-substituted copolymers apparently enhanced the electroluminescent performance of their polymeric light-emitting diodes (PLEDs). A diphenylvinyl-bearing copolymer (pDPV) PLED exhibited sky-blue EL ($\lambda_{\text{max}}^{\text{EL}} = 473$ nm, $\text{CIE}_{x,y} = 0.16, 0.28$) with peak luminous efficiency of 2.21 cd/A; a *N*-carbazole bearing copolymer (pCBZ) PLED displayed a blue EL ($\lambda_{\text{max}}^{\text{EL}} = 469$ nm, $\text{CIE}_{x,y} = 0.15, 0.22$) with peak luminous efficiency of 2.15 cd/A. OXD-7 (1,3-bis(2-(4-*tert*-butylphenyl)-1,3,4-oxadiazol-5-yl)benzene) as an electron-transporting dopant was found to improve the performance of PLED significantly. A better balanced hole/electron charge carrier was ascribed to electron-transporting, 1,3,4-oxadiazole-bearing copolymer (pOXD) PLED. It showed a very mild efficiency rolls off: only 0.13 cd/A luminous efficiency drops from current densities of 10–100 mA/cm², corresponding to EL brightness of 169–1558 cd/m².

Introduction

Blue-light-emitting polymers have been extensively studied due to practical applications of full-color flat-panel displays or renovated solid-state lightings (SSLs).¹ They can serve as the light-emitting layer or the host material for luminous dopants in generating other long-wavelength colors in polymer light-emitting diodes (PLEDs). Blue color fluorophores commonly consist of chemical structures like phenyl, carbazole, fluorene, or heterocyclic rings, such as thiophene, pyridine, and furan.¹ Over the past two decades, a variety of the wide-band-gap polymers with blue-light emission have been developed, they are poly(*p*-phenylene), poly(dibenzosilole),² polyfluorenes, polypyridines, and polycarbazoles, etc. For blue fluorophores, anthracene is the first reported organic material observed for electroluminescence (EL) in 1963 by Pope and co-workers.³ Since then, many anthracene derivatives have been developed and applied for organic light-emitting diodes (OLEDs) because of their pure blue fluorescence and high solution fluorescence quantum yields (Φ_{fs}). Among them, 9,10-substituted anthracene derivative has been one of practical chemical structures for blue-emitters⁴ or host materials for downhill energy transfer to green- or red-emitters.⁵ In the molecular design of these materials for OLEDs, electron/hole transporting^{4a,d,c} as well as bulky π -conjugated moieties^{4b,c} are often incorporated into the anthracene derivatives. Many of them exhibit excellent efficiencies. However, for PLEDs, few anthracene-based polymeric materials have shown satisfactory EL efficiency so far.^{6–9} The anthracene unit can be incorporated into the polymer chain through

several methods, such as the side-chain groups of the polymer.⁷ There are many more cases having an extension of the polymer chain through 9,10-linked anthrylene,⁶ but very few along 2,6-positions of anthracene derivatives.⁸ In spite of high solution fluorescence quantum yields (Φ_{f}), when fabricated into PLEDs, none of these anthracene-derived blue light-emitting polymers exhibited luminous efficiency more than 1 cd/A, and the electroluminescence of these polymers rarely exceeded 1000 cd/m². Moreover, either 9,10- or 2,6-linked anthrylene polymers often show red-shifting EL having downgrade blue color purity. Therefore, the development of efficient and bright anthracene-derived blue light-emitting polymers for PLEDs applications still remains a challenge.

In this work, we report a series of new 9,10-diphenylanthracene (DPA)-derived blue fluorescent copolymers. Since the extension of the copolymer chain is through the 2,6-positions of DPA, these copolymers enable the chemical grafting with hole-transporting, electron-transporting, or bulky π -conjugation moiety on DPA unit. In order to preserve the intrinsic wide-band-gap energy of DPA for blue EL, we adopt a dioctyl-substituted phenylene unit as the comonomer for the copolymerization with 2,6-linked anthrylene derivatives. Such phenylene unit plays a role of the π -conjugation twister between each 2,6-linked anthrylene unit in the polymer backbone. The synthesis, characterization, and EL properties of these novel blue light-emitting copolymers are reported herein. Influences of the substituted group, including hole injection/transport, electron injection/transport, and bulky moieties, on the EL performance of these blue light-emitting copolymers are also discussed. To the best of our knowledge, the EL performance of 2,6-linked anthrylenephylene copolymers reported here is one of the best among all anthracene-derived PLEDs reported so far. Our results also provide insightful

*Corresponding authors. E-mail: cchen@chem.sinica.edu.tw, chenct@ntu.edu.tw.

information about the judicious design of blue-light-emitting polymers based on DPA fluorophores for PLED applications.

Experimental Section

General. ^1H and ^{13}C NMR spectra were recorded on a Bruker AV-400 MHz or AV-500 MHz Fourier transform spectrometer at room temperature. Elemental analyses (on a Perkin-Elmer 2400 CHN elemental analyzer), electron ionization (EI), or fast atom bombardment (FAB) mass spectroscopy (MS) were performed by the Elemental Analyses and Mass Spectroscopic Laboratory, respectively, in-house service of the Institute of Chemistry, Academic Sinica. The number- and weight-average molecular weight of polymers were determined by gel permeation chromatography (GPC) on a Waters GPC-1515 with a 2414 refractive index detector, using THF as the eluent and polystyrene as the standard. UV-vis absorption spectra were recorded on a Hewlett-Packard 8453 diode array spectrophotometer. Photoluminescence (PL) spectra were recorded on a Hitachi fluorescence spectrophotometer F-4500. Glass transition temperatures (T_g 's) and thermal decomposition temperatures (T_d 's) of the copolymers were measured via differential scanning calorimetry (DSC) and thermogravimetric analysis (TGA) using Perkin-Elmer DSC-6 and TGA-7 analyzer systems, respectively. The temperatures at the intercept of the curves on the thermogram (endothermic, exothermic, or weight loss) and the leading baseline were taken as the estimates for the onset T_g and T_d . Both solution and solid-state fluorescence quantum yields of the copolymers were determined using the integrating sphere method described by de Mello et al.¹⁰

Materials. All chemicals were purchased from Aldrich and Acros Chemical Co. and were used without any further purification. All solvents such as toluene, DMSO, and THF were distilled after drying with appropriate drying agents. The dried solvents were stored over 4 Å molecular sieves before usage. Compounds 1,4-dibromo-2,5-diethylbenzene,¹¹ 1-bromo-3-iodobenzene,¹² 3,6-di-*tert*-butyl-9*H*-carbazole,¹³ 2,6-dibromoanthraquinone,¹⁴ and 1,1-diphenyl-2-(4-bromophenyl)ethane, BrDPV,¹⁵ were synthesized according to the literature methods.

2,2'-(2,5-Dioctyl-1,4-phenylene)bis(4,4,5,5-tetramethyl-1,3,2-dioxaborolane), DOPTMBO. A flask charged with 1,4-dibromo-2,5-diethylbenzene (4.58 g, 10.0 mmol), bis(pinacolato)-diboron (5.59 g, 22.0 mmol), $\text{PdCl}_2(\text{dppf})$ (0.44 g, 6 mol %), and potassium acetate (5.89 g, 60.0 mmol) in 60 mL of DMSO was stirred at 80 °C for 6 h under a nitrogen atmosphere. After cooling, the mixture was diluted with 50 mL of benzene and then washed with H_2O (3×50 mL). After drying over magnesium sulfate, the organic phase was evaporated under reduced pressure, and the residual solid was recrystallized from methanol to afford a white crystal (2.03 g, 37%). ^1H NMR (CDCl_3 , 400 MHz, δ /ppm): 7.50 (s, 2H), 2.78 (t, 4H, $J = 8.00$ Hz), 1.51–1.45 (m, 4H), 1.41–1.25 (m, 44H), 0.86 (t, 6H, $J = 6.80$ Hz). ^{13}C NMR (CDCl_3 , 400 MHz, δ /ppm): 146.1, 136.4, 130.4, 83.2, 35.5, 33.8, 31.9, 29.9, 29.5, 29.3, 24.8, 22.6, 14.1. HRMS (m/z): [M^+] calcd for $\text{C}_{34}\text{H}_{60}\text{B}_2\text{O}_4$ 554.4678; found 554.4677. Anal. Found (Calcd) for $\text{C}_{34}\text{H}_{60}\text{B}_2\text{O}_4$: C, 73.82 (73.65); H, 10.66 (10.91).

9-(3-Bromophenyl)-3,6-di-*tert*-butylcarbazole, BrCBZ. A mixture of 1-bromo-3-iodobenzene (5.47 g, 19.39 mmol), 3,6-di-*tert*-butyl-9*H*-carbazole (5.31 g, 19.00 mmol), copper powder (3.66 g, 58.17 mmol), and potassium carbonate (8.02 g, 58.17 mmol) in DMF (44 mL) was stirred at refluxing temperature for 24 h under a nitrogen atmosphere. After cooling to room temperature, the reaction mixture was diluted with ethyl acetate and filtered through Celite. The filtrate was poured into water and then extracted with ethyl acetate. The combined organic phase was washed with brine and dried over magnesium sulfate. The subjection of the crude mixture to silica gel chromatography (hexanes) afforded colorless oil (5.56 g, 68%). ^1H NMR (CDCl_3 , 500 MHz, δ /ppm): 8.10 (d, 2H, $J = 1.90$ Hz), 7.71 (t, 1H, $J = 1.89$ Hz), 7.54–7.48 (m, 2H), 7.46–7.41 (m, 3H), 7.33 (d, 2H, $J = 8.75$ Hz), 1.44 (s, 18H).

N-(3-Bromophenyl)-N-phenylnaphthalen-1-amine, BrNPA. A mixture of palladium acetate (0.09 g, 4 mol %), 1,1-bis-(diphenylphosphino)ferrocene (0.444 g, 8 mol %), sodium *tert*-butoxide (4.81 g, 50.0 mmol), *m*-dibromobenzene (3.54 g, 15 mmol), and *N*-phenyl-1-naphthylamine (2.19 g, 10.0 mmol) was dissolved in toluene (15 mL) and heated at 110 °C for 48 h under nitrogen. After cooling to room temperature, the solution was filtered through Celite. The organic layer was removed under reduced pressure, and the residue was purified by silica gel column chromatography using hexanes as an eluent to give the product (1.36 g, 36%). ^1H NMR (CDCl_3 , 400 MHz, δ /ppm): 7.87 (d, 2H, $J = 8.40$ Hz), 7.77 (d, 1H, $J = 8.20$ Hz), 7.48–7.43 (m, 2H), 7.38–7.34 (m, 1H), 7.30 (dd, 1H, $J = 7.32$ Hz, $J = 1.12$ Hz), 7.22–7.18 (m, 2H), 7.11–7.10 (m, 1H), 7.05 (dd, 2H, $J = 6.60$ Hz, $J = 1.16$ Hz), 7.00–6.97 (m, 3H), 6.84–6.81 (m, 1H).

3-Bromophenyltriphenylsilane, BrTPS. To a magnetically stirred solution of *m*-dibromobenzene (2.60 g, 11.0 mmol) in anhydrous THF (100 mL) was cooled to –78 °C, 7.20 mL of *n*-BuLi (1.6 M in hexane, 11.5 mmol) was added slowly under nitrogen. After stirred at –78 °C for 3 h, triphenylsilyl chloride (2.95 g, 10.0 mmol) was added into the solution in one portion. The reaction mixture was gradually allowed to warm up to room temperature during 16 h of stirring. The reaction mixture was poured into water, and then this aqueous solution was extracted with diethyl ether. The extracts were washed with water and dried over magnesium sulfate. The crude product was purified by silica gel column chromatography using hexanes as an eluent to obtain a white powder (2.75 g, 60%). ^1H NMR (CDCl_3 , 500 MHz, δ /ppm): 7.64 (t, 1H, $J = 1.10$ Hz), 7.55–7.51 (m, 7H), 7.46–7.41 (m, 4H), 7.38–7.35 (m, 6H), 7.22 (d, 1H, $J = 9.61$ Hz). ^{13}C NMR (CDCl_3 , 400 MHz, δ /ppm): 138.6, 137.8, 136.3, 134.8, 133.3, 132.7, 129.8, 129.6, 128.0, 127.8, 123.0. HRMS (m/z): [M^+] calcd for $\text{C}_{24}\text{H}_{19}\text{BrSi}$ 414.0439; found 414.0438.

5-(3-Bromophenyl)-1*H*-tetrazole, BrN4. 3-Bromobenzonitrile (10.92 g, 60 mmol) was added to a dried DMF (300 mL) solution containing sodium azide (19.50 g, 300 mmol) and ammonium chloride (16.05 g, 300 mmol). The mixture was slowly heated to refluxing temperature for 16 h under a nitrogen atmosphere. Excess salts remained as a suspension even at high temperature. After cooling the reaction mixture, it was then acidified with a 2 N HCl aqueous solution (attention: hydrazoic acid is formed!) until acidic conditions were reached, after which a white powder slowly appeared. The product was isolated by filtration and washed thoroughly with water to eliminate excess salts. After drying in a vacuum oven, the product was obtained as a white solid with quantitative yields. ^1H NMR (CDCl_3 , 400 MHz, δ /ppm): 8.25 (s, 1H), 8.03 (d, 1H, $J = 7.96$ Hz), 7.64 (d, 1H, $J = 7.52$ Hz), 7.40 (t, 1H, $J = 7.94$ Hz). HRMS (m/z): [M^+] calcd for $\text{C}_7\text{H}_5\text{BrN}_4$ 224.9776; found 224.9779.

2-(3-Bromophenyl)-5-(3-(trifluoromethyl)phenyl)-1,3,4-oxadiazole, BrOXD. 5-(3-Bromophenyl)-1*H*-tetrazole (11.41 g, 50.95 mmol) was dissolved in dried anisole (200 mL) containing 3-(trifluoromethyl)benzoyl chloride (10.63 g, 50.95 mmol). 2,4,6-Collidine (7.4 mL) was added dropwise to the mixture with stirring. After the addition of collidine, the solution was heated to reflux for 4 h under a nitrogen atmosphere. The solvent was removed under reduced pressure, and then the product was purified by silica gel column chromatography using hexanes containing 10% ethyl acetate as the eluent to obtain a white powder (13.12 g, 70%). ^1H NMR (CDCl_3 , 500 MHz, δ /ppm): 8.38 (s, 1H), 8.34 (d, 1H, $J = 7.96$ Hz), 8.29 (t, 1H, $J = 1.78$ Hz), 8.09 (d, 1H, $J = 7.86$ Hz), 7.82 (d, 1H, $J = 7.90$ Hz), 7.69 (t, 2H, $J = 7.91$ Hz), 7.26 (t, 1H, $J = 7.93$ Hz). ^{13}C NMR (CDCl_3 , 500 MHz, δ /ppm): 163.6, 134.9, 131.8 (q, $J_{\text{CF}} = 132$ Hz), 130.7, 130.1, 129.8, 129.7, 128.3 ($\times 2$), 125.5, 125.3, 124.5, 123.8, 123.7, 123.2, 122.4. HRMS (m/z): [M^+] calcd for $\text{C}_{15}\text{H}_8\text{BrF}_3\text{N}_2\text{O}$ 368.9850; found 368.9847. Anal. Found (Calcd) for $\text{C}_{15}\text{H}_8\text{BrF}_3\text{N}_2\text{O}$: C, 48.68 (48.81); H, 2.42 (2.18); N, 7.69 (7.59).

2,6-Dibromo-9,10-diphenylanthracene, Br₂DPA. To a solution of bromobenzene (9.36 g, 60.0 mmol) in anhydrous THF

(300 mL) at -78°C , 22.8 mL of *n*-BuLi (2.5 M in hexane, 57.0 mmol) was slowly added. The mixture was stirred at -78°C for 2 h, and then 2,6-dibromoanthraquinone (5.46 g, 15.0 mmol) was added into the mixture immediately. The resulting mixture was allowed to warm up to room temperature slowly and then stirred for 24 h. The reaction mixture was poured into water and then extracted with ethyl acetate. The combined organic extracts were washed with brine and dried over magnesium sulfate. After the organic solvent was removed under reduced pressure, the residue was purified by column chromatography on silica gel (ethyl acetate/hexanes, 1:4) to obtain the diol intermediate. A mixture of the diol intermediate, potassium iodide (4.98 g, 30.0 mmol), sodium hypophosphite hydrate (10.60 g, 100.0 mmol) was stirred in acetic acid (100 mL) at refluxing temperature for 16 h. After cooling to room temperature, the reaction mixture was poured into a mixture of ice and water. The precipitate was filtered and washed with water. The residue was purified by column chromatography on silica gel (dichloromethane/hexanes, 1:5) and then recrystallized from THF to afford a yellow powder (3.50 g, 48%). ^1H NMR (CDCl_3 , 500 MHz, δ/ppm): 7.80 (d, 2H, $J = 1.89$ Hz), 7.62–7.55 (m, 6H), 7.52 (d, 2H, $J = 9.47$ Hz), 7.42–7.40 (m, 4H), 7.36 (dd, 2H, $J = 9.50$ Hz, $J = 1.97$ Hz). ^{13}C NMR (CDCl_3 , 500 MHz, δ/ppm): 137.7, 136.8, 131.1, 130.8, 129.1, 128.9, 128.7, 128.1, 120.2. HRMS (m/z): [M^+] calcd for $\text{C}_{26}\text{H}_{16}\text{Br}_2$ 485.9619; found 485.9612. Anal. Found (Calcd) for $\text{C}_{26}\text{H}_{16}\text{Br}_2$: C, 63.94 (63.96); H, 3.35 (3.30).

2,6-Dibromo-9,10-bis(4-(2,2-diphenylvinyl)phenyl)anthracene, Br₂DPV. Br₂DPV was synthesized from 1,1-diphenyl-2-(4-bromophenyl)ethene (2.09 g, 6.27 mmol) and 2,6-dibromoanthraquinone (0.98 g, 2.67 mmol) by using a synthetic method similar to Br₂DPA. The desired product was obtained by silica gel flash column chromatography (dichloromethane/hexanes, 1:5) and then recrystallized from THF to afford a yellow powder (1.04 g, 46%). ^1H NMR (CDCl_3 , 500 MHz, δ/ppm): 7.76 (d, 2H, $J = 1.9$ Hz), 7.50 (d, 2H, $J = 9.3$ Hz), 7.39–7.41 (m, 8H), 7.29–7.36 (m, 16H), 7.23 (d, 2H, $J = 4.3$ Hz), 7.15 (d, 4H, $J = 8.14$ Hz), 7.12 (s, 2H). ^{13}C NMR (CDCl_3 , 500 MHz, δ/ppm): 143.6, 143.3, 140.3, 137.3, 136.6, 135.9, 130.8, 130.7, 130.4, 129.7, 129.1, 128.8, 128.7, 128.3, 127.7, 120.1. HRMS (m/z): [M^+] calcd for $\text{C}_{54}\text{H}_{36}\text{Br}_2$ 842.1184; found 842.1174. Anal. Found (Calcd) for $\text{C}_{54}\text{H}_{36}\text{Br}_2$: C, 76.77 (76.78); H, 4.31 (4.30).

9,9'-(3,3'-(2,6-Dibromoanthracene-9,10-diyl)bis(3,1-phenylene))-bis(3,6-di-*tert*-butyl-9H-carbazole), Br₂CBZ. Br₂CBZ was synthesized from 9-(3-bromophenyl)-3,6-di-*tert*-butylcarbazole, BrCBZ (5.28 g, 12.2 mmol), and 2,6-dibromoanthraquinone (1.46 g, 4.0 mmol) using a synthetic method similar to Br₂DPA. The desired product was obtained by silica gel flash column chromatography (dichloromethane/hexanes, 1:5) and then recrystallized from THF to afford a white powder (2.50 g, 60%). ^1H NMR (CDCl_3 , 500 MHz, δ/ppm): 8.12 (d, 4H, $J = 13.1$ Hz), 8.02 (s, 2H), 7.86–7.80 (m, 4H), 7.71 (d, 2H, $J = 9.3$ Hz), 7.65 (d, 2H, $J = 15.5$ Hz), 7.56–7.47 (m, 12H), 1.45 (s, 18H), 1.43 (s, 18H). ^{13}C NMR (CDCl_3 , 500 MHz, δ/ppm): 143.2, 139.3, 138.9, 138.8, 138.7, 135.9, 130.8, 130.2, 129.6, 128.9, 128.7, 128.6, 126.0, 123.8, 123.6, 120.7, 116.3, 109.2, 31.9. HRMS (m/z): [M^+] calcd for $\text{C}_{66}\text{H}_{62}\text{Br}_2\text{N}_2$ 1040.3280; found 1040.3293. Anal. Found (Calcd) for $\text{C}_{66}\text{H}_{62}\text{Br}_2\text{N}_2$: C, 75.75 (76.00); H, 6.07 (5.99); N, 2.72 (2.69).

5,5'-(3,3'-(2,6-Dibromoanthracene-9,10-diyl)bis(3,1-phenylene))-bis(2-(3-(trifluoromethyl)phenyl)-1,3,4-oxadiazole), Br₂OXD. Br₂OXD was synthesized from 2-(3-bromophenyl)-5-(3-(trifluoromethyl)phenyl)-1,3,4-oxadiazole, BrOXD (1.104 g, 3.00 mmol), and 2,6-dibromoanthraquinone (0.364 g, 1.0 mmol) using a synthetic method similar to Br₂DPA. The desired product was obtained by silica gel flash column chromatography (dichloromethane/ethyl acetate, 1:5) and then recrystallized from THF to afford a white powder (1.26 g, 57%). ^1H NMR (CDCl_3 , 500 MHz, δ/ppm): 8.42 (t, 2H, $J = 6.5$ Hz), 8.34 (d, 2H, $J = 6.5$ Hz), 8.31 (d, 2H, $J = 7.5$ Hz), 8.22 (d, 2H, $J = 14.0$ Hz), 7.84 (q, 2H, $J = 7.0$ Hz), 7.74–7.77 (m, 4H), 7.63–7.69 (m, 4H), 7.51 (d, 2H, $J = 9.5$ Hz),

7.41 (d, 2H, $J = 9.5$ Hz). ^{13}C NMR (CDCl_3 , 500 MHz, δ/ppm): 164.7, 163.6, 138.9, 135.6, 134.6, 134.5, 131.9 (q, $J_{\text{CF}} = 132$ Hz), 130.8, 130.1, 129.9, 129.8 ($\times 2$), 129.3, 129.2, 128.7, 128.5, 128.4, 127.0, 124.6, 124.4, 124.3, 123.8, 122.4, 120.9. HRMS (m/z): [M^+] calcd for $\text{C}_{44}\text{H}_{22}\text{Br}_2\text{F}_6\text{N}_4\text{O}_2$ 910.0015; found 910.0014. Anal. Found (Calcd) for $\text{C}_{44}\text{H}_{22}\text{Br}_2\text{F}_6\text{N}_4\text{O}_2$: C, 57.94 (57.92); H, 2.51 (2.43); N, 6.06 (6.14).

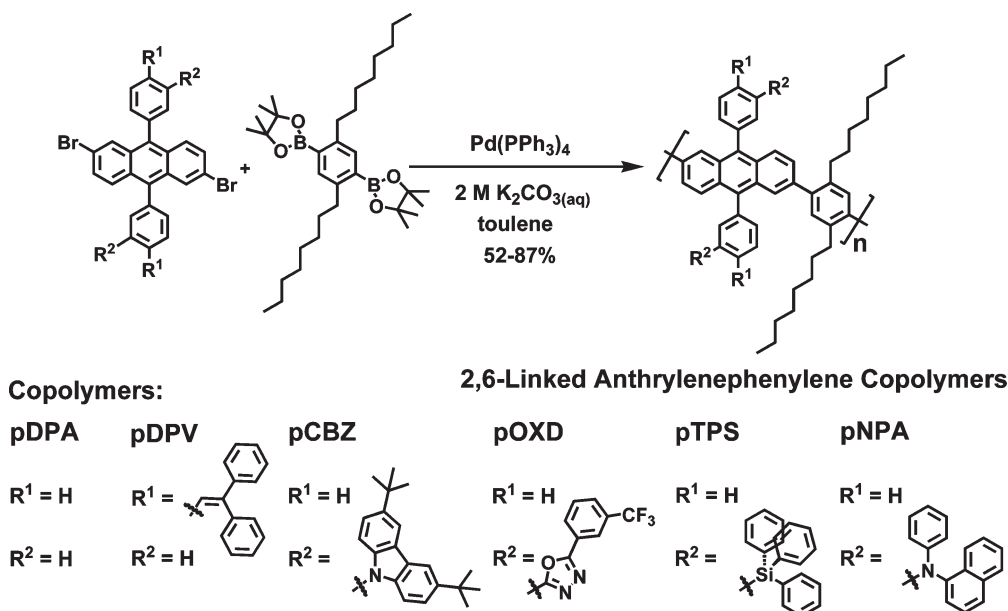
(3,3'-(2,6-Dibromoanthracene-9,10-diyl)bis(3,1-phenylene))-bis(triphenylsilane), Br₂TPS. Br₂TPS was synthesized from 3-bromophenyltriphenylsilane, BrTPS (2.75 g, 6.6 mmol), and 2,6-dibromoanthraquinone (0.80 g, 2.2 mmol) using a synthetic method similar to Br₂DPA. The desired product was obtained by silica gel flash column chromatography (dichloromethane/hexanes, 10:1) and then recrystallized from THF to afford a pale yellow powder (0.36 g, 40%). ^1H NMR (CDCl_3 , 400 MHz, δ/ppm): 7.85 (s, 2H), 7.71 (dd, 2H, $J = 6.8$ Hz, $J = 0.4$ Hz), 7.66 (d, 2H, $J = 9.2$ Hz), 7.63–7.58 (m, 14H), 7.55 (d, 2H, $J = 9.6$ Hz), 7.42–7.34 (m, 22H). ^{13}C NMR (CDCl_3 , 400 MHz, δ/ppm): 138.8, 137.0, 136.8, 136.4, 136.3, 136.2, 136.0, 135.1, 135.0, 133.9, 133.8, 132.4, 130.9, 129.7, 129.1, 128.8, 128.7, 128.3, 128.2, 128.1, 128.0, 127.9, 120.2. HRMS (m/z): [M^+] calcd for $\text{C}_{62}\text{H}_{44}\text{Br}_2\text{Si}_2$ 1002.1348; found 1002.1351. Anal. Found (Calcd) for $\text{C}_{62}\text{H}_{44}\text{Br}_2\text{Si}_2$: C, 73.85 (74.10); H, 4.62 (4.41).

***N,N'*-(3,3'-(2,6-Dibromoanthracene-9,10-diyl)bis(3,1-phenylene))-bis(*N*-phenyl-naphthalen-1-amine), Br₂NPA.** Br₂NPA was synthesized from *N*-(3-bromophenyl)-*N*-phenyl-naphthalen-1-amine, BrNPA (1.12 g, 3.01 mmol), and 2,6-dibromoanthraquinone (0.364 g, 1.0 mmol) using a similar method for DiBrDPA. The desired product was obtained by silica gel flash column chromatography (dichloromethane/hexanes, 1:10) as a bright-yellow powder (0.49 g, 53%). ^1H NMR (CDCl_3 , 500 MHz, δ/ppm): 7.99 (t, 2H, $J = 9.0$ Hz), 7.80–7.84 (m, 4H), 7.68–7.72 (m, 4H), 7.35–7.48 (m, 12H), 7.13–7.28 (m, 12H), 6.84–6.96 (m, 6H). ^{13}C NMR (CDCl_3 , 400 MHz, δ/ppm): 148.9, 148.1, 148.0, 143.4, 143.3, 138.4, 136.5, 135.3, 131.0, 130.5, 129.4, 129.2, 128.9, 128.7, 128.6, 128.5, 128.4, 127.1, 126.6, 126.5, 126.3, 126.2, 126.1, 124.2, 124.1, 124.0, 123.9, 122.6, 122.5, 122.3, 120.6, 120.5, 120.0. HRMS (m/z): [M^+] calcd for $\text{C}_{58}\text{H}_{38}\text{Br}_2\text{N}_2$ 920.1402; found 920.1412. Anal. Found (Calcd) for $\text{C}_{58}\text{H}_{38}\text{Br}_2\text{N}_2$: C, 74.09 (75.49); H, 4.17 (4.15); N, 3.19 (3.04).

Copolymer pDPA. Aqueous potassium carbonate (2.0 M, 5.0 mL) and three drops of phase transfer reagent Aliquat 336 were added to a mixture of monomers, Br₂DPA (0.49 g, 1.0 mmol) and 2,2'-(2,5-diocetyl-1,4-phenylene)bis(4,4,5,5-tetramethyl-1,3,2-dioxaborolane) (0.55 g, 1.0 mmol), in freshly distilled toluene (20.0 mL). The mixture was degassed by the freeze–pump–thaw method, and then Pd(PPh_3)₄ (12.0 mg, 1.0 mol %) was added under a nitrogen atmosphere. The mixture was vigorously stirred at 85–90 $^{\circ}\text{C}$ for more than 48 h under a nitrogen atmosphere. Polymer end-groups were then capped by heating the mixture at 85–90 $^{\circ}\text{C}$ for 12 h with phenylboronic acid (0.24 g) and then for another 12 h with 1-bromo-4-*tert*-butylbenzene (0.43 g). After cooling to room temperature, the mixture was poured into a solution (400 mL) of methanol and deionized water (10:1) with vigorous stirring. The resulting precipitate was isolated by filtration and redissolved in chloroform. It was then further purified by a short column packed with neutral aluminum oxide. The polymer solution was precipitated in acetone/methanol (volume ratio = 1:1), and the resulting copolymer pDPA was obtained as a pale yellow powder with isolated yields of 87% (0.55 g). ^1H NMR (CDCl_3 , 400 MHz, δ/ppm): 7.71–7.65 (m, 4H), 7.57–5.51 (m, 10H), 7.36–7.31 (m, 2H), 7.12 (s, 2H), 2.50 (s, 4H), 1.30 (s, 4H), 1.25–1.20 (m, 20H), 0.79 (t, 6H, $J = 7.0$ Hz). ^{13}C NMR (CDCl_3 , 400 MHz, δ/ppm): 140.7, 139.0, 138.0, 137.8, 137.0, 131.3, 131.1, 129.6, 129.2, 128.5, 127.7, 127.5, 126.7, 126.6, 32.7, 31.9, 31.4, 29.6, 29.3, 29.2, 22.6, 14.1. Anal. Found (Calcd): C, 89.35 (91.37); H, 8.26 (8.63).

Copolymer pDPV. pDPV was obtained as a yellow powder with isolated yields of 69% (0.68 g). It was prepared from the reaction of Br₂DPV (0.82 g, 1.0 mmol) and 2,2'-(2,5-diocetyl-1,4-phenylene)bis(4,4,5,5-tetramethyl-1,3,2-dioxaborolane) (0.55 g,

Scheme 1. Synthesis and Chemical Structures of 2,6-Linked Anthrylenephénylene Copolymers



1.0 mmol) according to the procedure described for the synthesis of pDPA. ^1H NMR (CDCl_3 , 400 MHz, δ/ppm): 7.61–7.81 (m, 4H), 7.23–7.50 (m, 26H), 6.96–7.15 (m, 8H), 2.42–2.63 (m, 4H), 1.32–1.47 (m, 4H), 1.09–1.30 (m, 20H), 0.71–0.81 (m, 6H). ^{13}C NMR (CDCl_3 , 400 MHz, δ/ppm): 143.4, 143.1, 140.4, 140.1, 137.8, 137.4, 136.7, 131.1, 130.4, 129.5, 129.1, 128.7, 128.2, 127.9, 127.6, 127.5, 126.6, 32.8, 31.8, 31.4, 29.6, 29.3, 29.2, 22.6, 14.1. Anal. Found (Calcd): C, 90.87 (92.45); H, 7.47 (7.55).

Copolymer pCBZ. pCBZ was obtained as a slight yellow powder with isolated yields of 68% (0.81 g). It was prepared from the reaction of Br_2CBZ (1.04 g, 1.0 mmol) and 2,2'-(2,5-dioctyl-1,4-phenylene)bis(4,4,5,5-tetramethyl-1,3,2-dioxaborolane) (0.55 g, 1.0 mmol) according to the procedure described for the synthesis of pDPA. ^1H NMR (CDCl_3 , 500 MHz, δ/ppm): 8.13–8.07 (m, 4H), 7.92–7.85 (m, 4H), 7.82–7.70 (m, 6H), 7.59–7.42 (m, 8H), 7.41–7.33 (m, 4H), 7.21 (s, 2H), 2.54 (s, 4H), 1.45–1.33 (m, 40H), 1.08–0.84 (m, 20H), 0.66–0.61 (m, 6H). ^{13}C NMR (CDCl_3 , 500 MHz, δ/ppm): 143.0, 140.7, 138.9, 138.8, 138.6, 138.0, 136.4, 131.2, 129.9, 129.7, 129.5, 129.2, 128.9, 128.2, 127.4, 126.5, 125.4, 123.5, 116.2, 109.4, 34.7, 32.8, 32.4, 32.0, 31.7, 31.4, 29.5, 29.2, 29.1, 29.0, 22.5, 14.0. Anal. Found (Calcd): C, 88.49 (89.14); H, 8.37 (8.50); N, 2.74 (2.36).

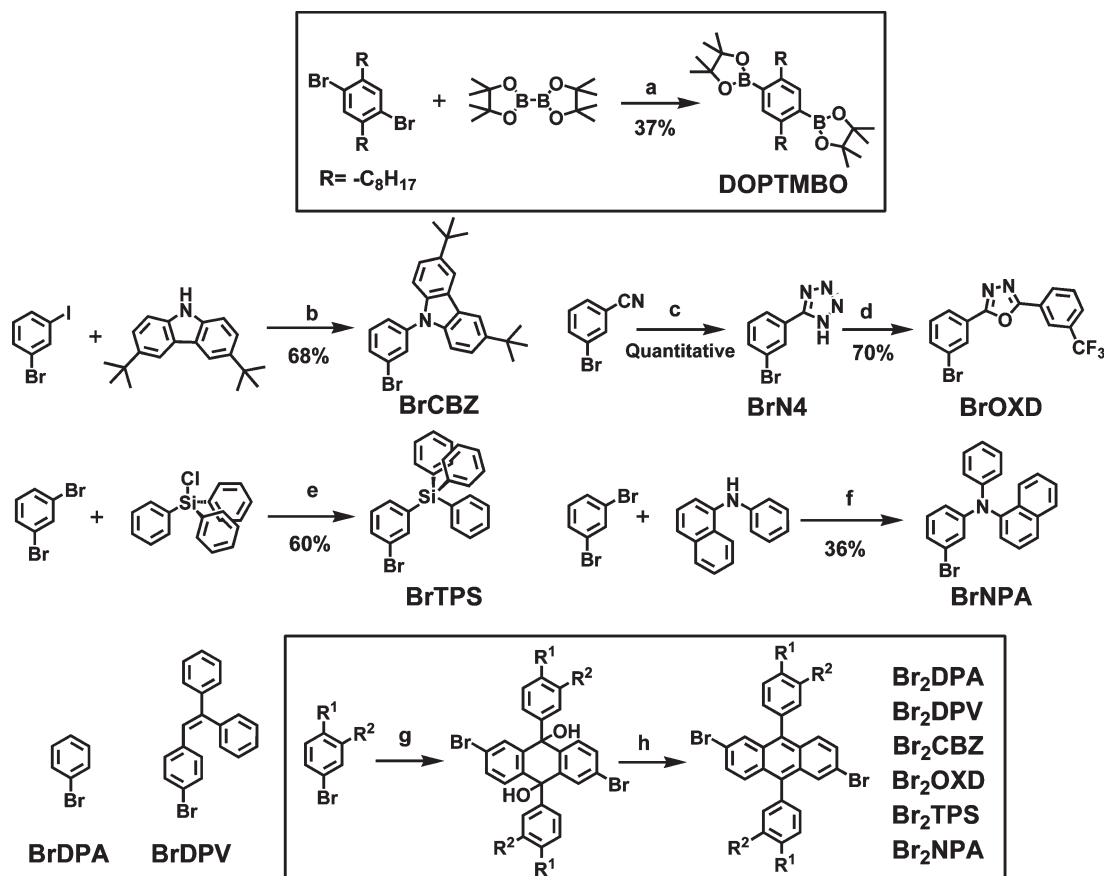
Copolymer pOXD. pOXD was obtained as a pale yellow powder with isolated yields of 84% (0.89 g). It was prepared from the reaction of Br_2OXD (0.91 g, 1.0 mmol) and 2,2'-(2,5-dioctyl-1,4-phenylene)bis(4,4,5,5-tetramethyl-1,3,2-dioxaborolane) (0.55 g, 1.0 mmol) according to the procedure described for the synthesis of pDPA. ^1H NMR (CDCl_3 , 400 MHz, δ/ppm): 8.24–8.38 (m, 8H), 7.58–7.83 (m, 12H), 7.32–7.41 (m, 2H), 7.08 (s, 2H), 2.36–2.56 (m, 4H), 1.15–1.38 (m, 4H), 0.85–1.13 (m, 20H), 0.62–0.71 (m, 6H). Anal. Found (Calcd): C, 74.83 (75.12); H, 5.57 (5.73); N, 5.35 (5.31).

Copolymer pTPS. pTPS was obtained as an off-white powder with isolated yields of 52% (0.45 g). It was prepared from the reaction of Br_2TPS (0.75 g, 0.75 mmol) and 2,2'-(2,5-dioctyl-1,4-phenylene)bis(4,4,5,5-tetramethyl-1,3,2-dioxaborolane) (0.42 g, 0.75 mmol) according to the procedure described for the synthesis of pDPA. ^1H NMR (CDCl_3 , 400 MHz, δ/ppm): 7.74–7.86 (m, 4H), 7.47–7.68 (m, 24H), 7.34–7.43 (m, 6H), 7.10–7.33 (m, 12H), 2.35–2.60 (m, 4H), 1.19–1.31 (m, 4H), 0.88–1.10 (m, 20H), 0.59–0.72 (m, 6H). ^{13}C NMR (CDCl_3 , 500 MHz, δ/ppm): 147.5, 144.2, 140.9, 139.1, 138.8, 138.5, 138.4, 137.9, 137.6, 137.3, 137.1, 137.0, 136.4, 136.3, 135.6, 134.7, 134.1, 134.0,

133.9, 132.8, 131.2, 131.0, 129.7, 129.5, 129.4, 129.3, 129.2, 128.0, 127.9, 126.9, 126.7, 126.6, 126.4, 126.3, 35.6, 33.6, 32.7, 31.9, 31.8, 31.5, 31.3, 29.9, 29.7, 29.5, 29.4, 29.2, 29.1, 24.9, 22.7, 22.5, 14.1, 13.9. Anal. Found (Calcd): C, 84.84 (87.90); H, 7.06 (7.20).

Copolymer pNPA. pNPA was obtained as a slight yellow powder with isolated yields of 77% (0.34 g). It was prepared from the reaction of Br_2NPA (0.38 g, 0.41 mmol) and 2,2'-(2,5-dioctyl-1,4-phenylene)bis(4,4,5,5-tetramethyl-1,3,2-dioxaborolane) (0.23 g, 0.41 mmol) according to the procedure described for the synthesis of pDPA. ^1H NMR (CDCl_3 , 400 MHz, δ/ppm): 7.91–8.08 (m, 2H), 7.59–7.89 (m, 6H), 7.26–7.52 (m, 12H), 6.95–7.23 (m, 18H), 6.78–6.91 (m, 2H), 2.31–2.71 (m, 4H), 1.31–1.49 (m, 4H), 0.92–1.28 (m, 20H), 0.68–0.86 (m, 6H). ^{13}C NMR (CDCl_3 , 400 MHz, δ/ppm): 148.8, 148.2, 143.6, 141.0, 139.9, 137.9, 137.1, 135.3, 131.1, 129.1, 128.4, 127.1, 126.3, 124.6, 124.3, 122.6, 121.9, 120.6, 32.9, 31.8, 31.5, 29.7, 29.3, 29.1, 24.9, 22.6, 14.1. Anal. Found (Calcd): C, 86.49 (90.18); H, 7.00 (7.19); N, 3.07 (2.63).

Fabrication and Characterization of PLED. The ITO glass plate was exposed on oxygen plasma at a power of 50 W for 5 min after ultrasonically in detergent, deionized water, acetone, and isopropyl alcohol. A hole injection layer, poly(3,4-ethylenedioxythiophene):poly(styrenesulfonate) (PEDOT:PSS) (Baytron P VPCH 8000 from H. C. Starck), was spin-coated on the ITO glass to achieve a thickness around 50 nm. The film was baked at 200 °C for 5 min in a nitrogen glovebox after drying at 140 °C for 10 min in the air. Inside a nitrogen glovebox, a hole-transporting material, poly(*N*-vinylcarbazole) (PVK), dissolved in chlorobenzene (10 mg mL^{-1}) was spin-coated on top of PEDOT:PSS layer to achieve a thickness about 25 nm. In order to reduce intermixing upon spin-coating the light-emitting copolymer, PVK layer was bake-dried at 200 °C for 1 h. On top of ITO/PEDOT:PSS/PVK, a thin layer (~100 nm) of light-emitting copolymer was spin-coated from its chlorobenzene solution (10 mg mL^{-1}), and the copolymer layer was bake-dried at 140 °C for 1 h inside the nitrogen glovebox. The hole-blocking/electron-transporting layer, 2,2',2''-(1,3,5-phenylene)tris(1-phenyl-1*H*-benzimidazole) (TPBI), was deposited by vacuum thermal deposition (8×10^{-6} Torr) to achieve a thickness of 25 nm. Finally, a thin layer of electron-injection layer, LiF (about 1.0 nm), and a layer of aluminum (120 nm) were directly vacuum-deposited thereon as the cathode of the devices. The active areas of the devices were 4 mm^2 , and a glass substrate was used to encapsulate the device in a nitrogen-filled glovebox (with O_2 and H_2O

Scheme 2. Preparation of DOPTMBO, BrCBZ, BrOXD, BrTPS, and BrNPA, and Six 2,6-Dibromosubstituted DPA Derived Monomers^a

^a Reagents and conditions: (a) PdCl₂(dppf), KOAc, DMSO, 80 °C; (b) Cu, K₂CO₃, DMF, reflux; (c) NaN₃, NH₄Cl, DMF, reflux; (d) 3-(trifluoromethyl)benzoyl chloride, 2,4,6-collidine, anisole, reflux; (e) *n*-BuLi, THF, −78 °C, 1 h; (f) Pd(OAc)₂, dppf, NaO^tBu, toluene, 110 °C; (g) i: *n*-BuLi, THF, −78 °C, 1 h; ii: 2,6-dibromoanthraquinone, −78 °C ~ rt; (h) KI, NaH₂PO₂·xH₂O, HOAc, reflux, 16 h.

concentration below 0.1 ppm). Current–voltage–luminance characteristics of the devices were measured under ambient conditions using a Keithley 2400 SourceMeter and a PR-650 SpectraScan spectrophotometer (Photo Research), both of which were computer controlled with a Labview program.

Results and Discussion

Synthesis and Characterization. As shown in Scheme 1, all new 2,6-linked diphenylanthracene-based copolymers were synthesized through the Suzuki cross-coupling reactions in good yields from substituted diphenylanthracene monomer and comonomer DOPTMBO, 2,2'-(2,5-diocetyl-1,4-phenylene)-bis(4,4,5,5-tetramethyl-1,3,2-dioxaborolane). DOPTMBO was synthesized from 1,4-dibromo-2,5-diocetylbenzene and bis(pinacolato)diboron catalyzed by PdCl₂(dppf) (dppf = 1,1'-bis(diphenylphosphino)ferrocene) with moderate yields (Scheme 2). In addition to the inhibition of emission wavelength from red-shifting, comonomer DOPTMBO was chosen to solubilize 2,6-linked anthracene-based copolymers. Substituted diphenylanthracene monomers, Br₂DPA, Br₂DPV, Br₂CBZ, Br₂OXD, Br₂TPS, and Br₂NPA, were synthesized from 2,6-dibromoanthraquinone¹⁴ following pertinent literature procedure in 40–60% isolated yields.¹⁶ Para-substituted diphenylvinylbromobenzene precursor, BrDPV, is a known compound which was synthesized according to the literature procedures.¹⁵ Previously unknown meta-substituted bromobenzene BrCBZ, BrOXD, BrTPS, and BrNPA were prepared via various synthetic routes shown in Scheme 2. Comonomer DOPTMBO and six 2,6-dibromo-substituted DPA derived monomers were characterized with

elemental analysis, ¹H/¹³C NMR, and HRMS for structural identification and purity check. Except for HRMS, a similar set of structure examination was applied to the six copolymers reported herein.

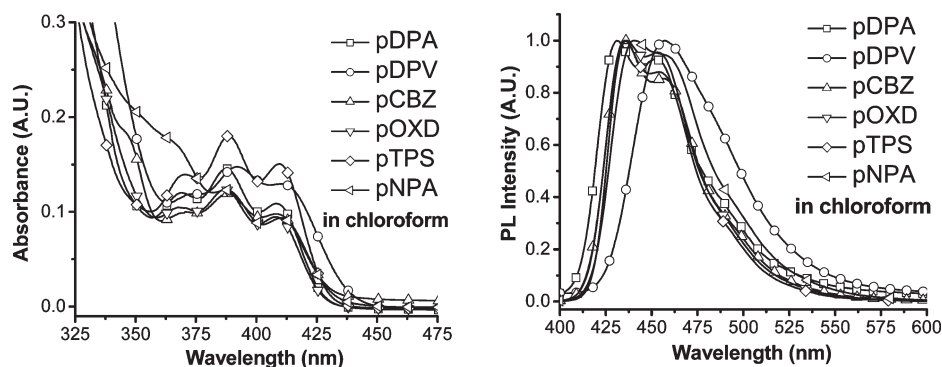
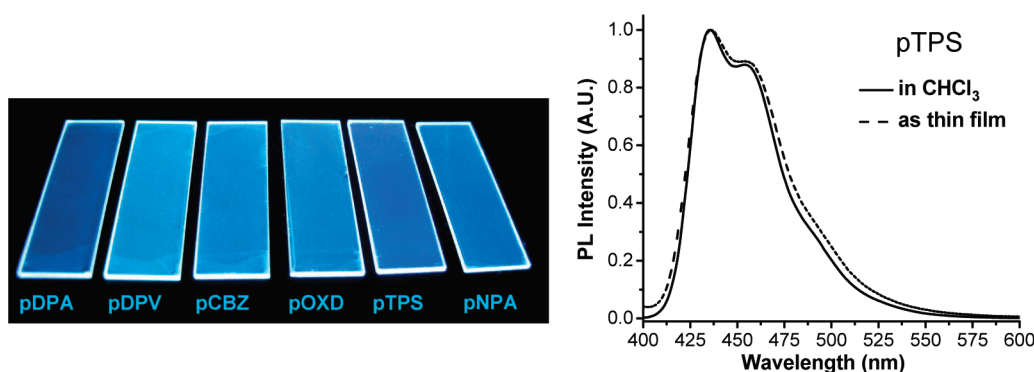
As data shown in Table 1, these copolymers have weight-average molecular weights (*M_w*) of 5300–46 200 with polydispersity indices (PDI, *M_w*/*M_n*) of 1.40–2.39. Except for pTPS, *M_w*s of these copolymers are higher than 10 000 g/mol. The significantly smaller *M_w* of pTPS may probably due to the steric hindrance caused by the bulky meta-substituted-triphenylsilane preventing its copolymer formation. The thermal properties of these copolymers were evaluated by TGA and DSC measurements under a nitrogen atmosphere (Table 1). All of these copolymers exhibit good thermal stability with decomposition temperatures (*T_d*s) above 400 °C which are determined by 5% weight loss of the copolymer. These copolymers exhibit relatively high glass-transition temperatures (*T_g*s) above 320 °C due to the rigid polycyclic aromatic hydrocarbon (PAH) backbone. This ensures the morphological stability of these copolymers fabricated as thin films. *T_g*s of 2,6-linked 9,10-diphenylanthracene copolymers have not been reported in the literature so far.^{8,16a,17}

Photoluminescent Characterization. Figure 1 shows the UV–vis absorption and fluorescence spectra of these copolymers in the dilute solution of chloroform. The absorption peaks around 360–430 nm with a characteristic feature of vibronic absorption are attributed to the π to π* transition of anthracene moiety,¹⁸ which is the main π-conjugation moiety responsible for emission (fluorescence). Except for pDPV,

Table 1. Molecular Weight, Thermal, and Photophysical Characterizations of Copolymers

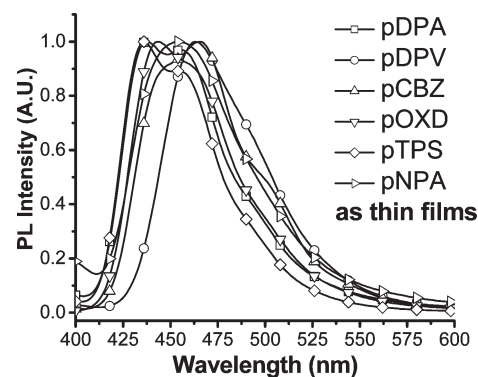
	$M_w^a (\times 10^4)$	$M_n^a (\times 10^4)$	PDI ^a	T_g^b (°C)	T_d (°C)	$\lambda_{max}^{FL}, \Phi_f^b$ fwhm ^c (nm, %, nm) ^d	$\lambda_{max}^{FL}, \Phi_f^b$ fwhm ^c (nm, %, nm) ^e
pDPA	3.7	1.71	2.16	328	430	431 (452), 73, 58	438 (456), 23, 60
pDPV	2.73	1.56	1.75	327	418	457, 85, 60	463, 20, 59
pCBZ	1.02	0.72	1.4	326	435	436 (456), 84, 53	466, 37, 68
pOXD	4.62	1.93	2.39	326	444	436 (454), 66, 51	444, 27, 59
pTPS	0.53	0.43	1.22	324	467	436 (455), 86, 50	436 (456), 62, 55
pNPA	1.1	0.66	1.67	325	407	441 (458), 34, 58	454, 20, 68

^a Analytical GPC was obtained in tetrahydrofuran (THF) using polystyrene as standard. ^b Using 9,10-diphenylanthracene as the standard reference ($\Phi_f = 0.96$). ^c Fwhm is the full width at half-maximum of emission bands. ^d In chloroform. ^e As thin films spin-coated from chlorobenzene solution.

**Figure 1.** Normalized absorption (left) and emission (right) spectra of copolymers in chloroform.**Figure 2.** Left: fluorescence images of copolymers as spin-coated thin films on quartz substrate. Right: normalized emission spectra of pTPS in chloroform solution and as thin film.

these copolymers exhibit essentially same fluorescence spectra in the deep blue area with two to three vibronic emission bands extended into long wavelength region of the visible spectrum. In addition to the less discernible vibronic emission side bands, pDPV shows the most red-shifted wavelength λ_{max}^{FL} of 457 nm in solution. This may be due to the π -conjugation nature of the diphenylvinyl substituent on the para-position of 9,10-diphenylanthracene.

Vision-wise, all copolymers exhibited blue to sky blue fluorescence in the thin film state (Figure 2, left). Spectroscopy-wise, compared with those in solution, all copolymers displayed a slight red-shifted fluorescent emission with less than 10 nm of red-shifting wavelength ($\Delta\lambda$), except for pCBZ ($\Delta\lambda = 30$ nm) and pNPA ($\Delta\lambda = 14$ nm) (Table 1 and Figure 3). This is a good indication of limited conformation change for the π -conjugated polymer backbone from solution to thin film state. Especially for the fluorescence spectra of pTPS in dilute solution and in the thin film are almost identical with $\Delta\lambda$ only 1 nm (Figure 2, right). This can be rationalized by the inhibition of the intermolecular π - π interactions among polymer chains due to the bulky tetraphenylsilane molecular structure.

**Figure 3.** Normalized emission spectra of copolymers in thin film state.

On the other hand, a bathochromic shift of the emission spectra was observed for the monomer Br₂NPA in solutions with increasing solvent polarity (Figure 4). Such solvatochromism usually happen to molecules with the polarity high in the excited state but low in the ground state. However, no solvatochromic shift was observed for the copolymer pNPA

in different solutions with varied polarity. This result implies that a molecular dipole moment is significant in the excited state of Br₂NPA, and it may be ascribed to the donor (diarylamine substituents)–acceptor (anthracene moiety) electron transfer character of Br₂NPA. For copolymer pNPA, such dipole is significantly reduced by the disoriented dipole in various directions along the whole π -conjugated polymer backbone. Molecular dipoles have been verified as an adverse effect on photoluminescence or electroluminescence.¹⁹ Similar character of electron transfer (judged by the shifting of emission wavelength in solution) was not observed for another arylamine-bearing DPA moiety Br₂CBZ. This is consistent with the exceptionally low solution fluorescence quantum yield (Φ_f) happened on pNPA instead of pCBZ (Table 1).

Comparison of these copolymers in solution and in thin film state reveals that all six copolymers suffer from medium to strong fluorescence quenching in solid states (Table 1). In

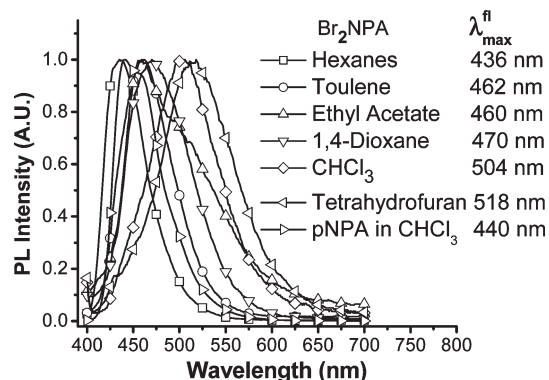


Figure 4. Normalized emission spectra of monomer Br₂NPA in hexanes, toluene, ethyl acetate, 1,4-dioxane, chloroform, tetrahydrofuran, and pNPA in chloroform.

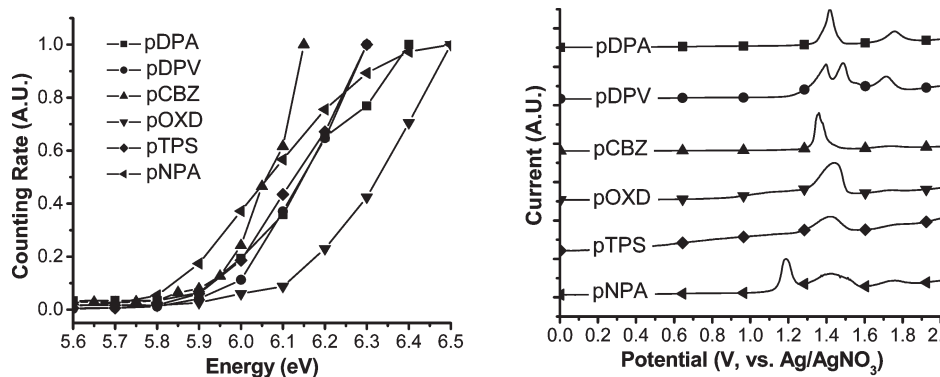


Figure 5. Low-energy photoelectron spectra of copolymers as solid thin films (left) and differential pulsed voltammograms of copolymers coated on glassy carbon electrodes in acetonitrile containing 0.1 M *n*-Bu₄NClO₄ at a scan rate of 100 mV s^{−1} (right).

Table 2. Electrochemical Properties and Energy Levels of the Copolymers

	E_g^a (eV)	$E_{\text{oxd},1}^{\text{DPV } b}$ (V)	HOMO ^{DPV c} (eV)	LUMO ^{DPV d} (eV)	HOMO ^{AC-2 e} (eV)	LUMO ^{AC-2 d} (eV)
pDPA	2.84	1.42	−5.79	−2.95	−5.89	−3.05
pDPV	2.76	1.4	−5.77	−3.01	−5.85	−3.09
pCBZ	2.83	1.36	−5.73	−2.9	−5.79	−2.96
pOXD	2.83	1.44	−5.81	−2.98	−5.99	−3.16
pTPS	2.87	1.43	−5.8	−2.93	−5.88	−3.01
pNPA	2.77	1.19	−5.56	−2.79	−5.76	−2.99

^a E_g is the energy band gap estimated from the low-energy edge of the absorption spectra from the polymer thin film. ^b The first oxidation potential obtained by differential pulsed voltammetry from the polymer thin film on a glassy carbon rod working electrode. ^c HOMO = $-4.8 \text{ eV} - e(E_{\text{oxd},1} - E_{\text{oxd,ferrocene}})$, where $E_{\text{oxd,ferrocene}}$ is the oxidation potential of ferrocene (0.43 V vs Ag/AgNO₃) determined by differential pulsed voltammetry in a 0.1 M solution of *n*-Bu₄NClO₄ in acetonitrile. ^d LUMO = HOMO + E_g . ^e HOMO energy level was determined by low-energy photoelectron spectrometer (Riken-Keiki AC-2).

chloroform solution, all copolymers have reasonably high 66–86%, except relatively low 34% of pNPA. The relatively low Φ_f of pNPA may be attributed to the above-mentioned donor–acceptor electron transfer character between naphthylphenyl amine and anthracene moieties. In the solid state, pTPS possesses a small fluorescence quenching with Φ_f as high as 62%, the highest among all copolymers. Relatively slight solid state fluorescence quenching was also observed for pCBZ in thin film state (Φ_f = 37%). The common structural feature of pTPS and pCBZ is the sterically hindered substituent on the anthracene-based 2,6-linked polyanthrylenephenylene backbone. The bulky substituents effectively prevent the polymer chain from π – π interactions and alleviate the solid-state fluorescence quenching, which is a common problem of anthracene-based fluorophores^{4b,d} or polymers.

Energy Levels Determination. The energy level of OLED materials is an important parameter that governs the efficiency of charge injection and cross-layer charge transport of holes or electrons. A low-energy photoelectron spectrometer (Riken-Keiki AC-2) was employed to estimate ionization potentials of these copolymers, which would be referred to the energy level of the highest occupied molecular orbitals (HOMOs). The HOMO energy levels were measured from copolymers in thin film state, which were prepared by spin-coating copolymer solutions (in chlorobenzene) on quartz plates. As shown in Figure 5 (left) and Table 2, HOMO energy levels of these copolymers were found to be around 5.76–5.99 eV below vacuum level. This difference can be attributed to the electron-donating ability from different charge-transporting substituents on the 9,10-diphenylanthracene moiety. For example, with the strong electron-donating diarylamine, pNPA possesses the lowest HOMO energy level among these copolymers.

Since the magnitude of the electrochemical oxidation potential reflects the ease of removing electrons from the HOMO, we can easily differentiate the electron-donating

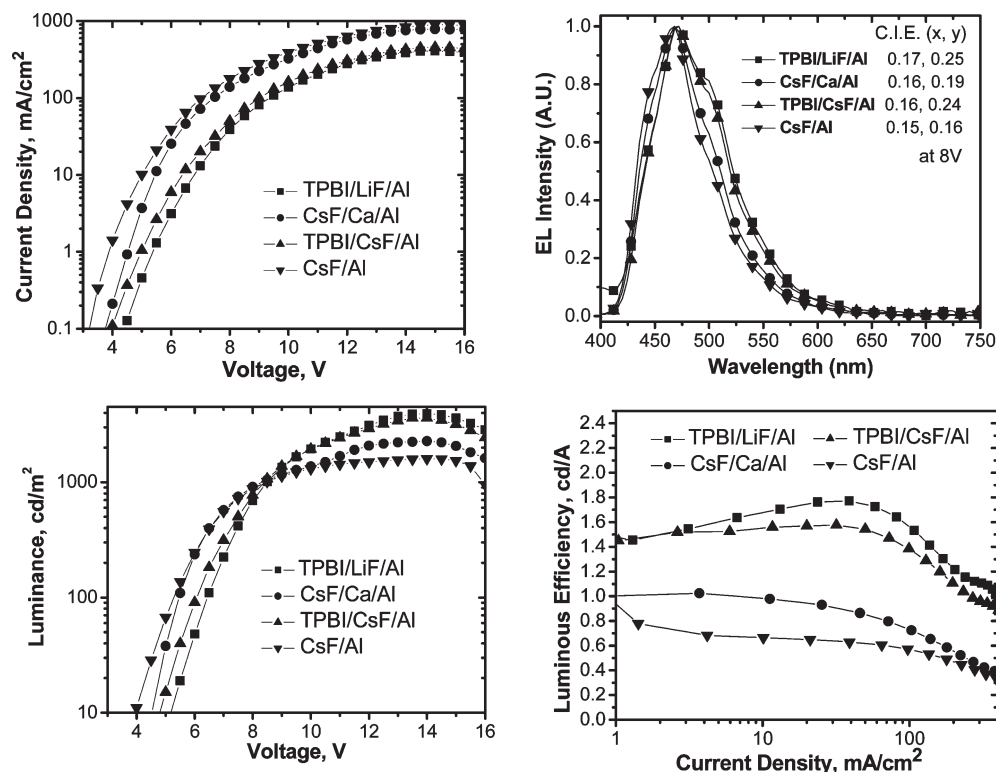


Figure 6. Electroluminescence (EL) characteristics of pOXD with the device configuration ITO/PEDOT:PSS/PVK/pOXD/cathodes.

ability of these copolymers via the electrochemical method. Additional data provided by differential pulsed voltammetry (DPV) have been used to show the electron-donating ability of these copolymers. Basically, a similar trend of the HOMO energy levels, determined by DPV, was comparable with those measured by AC-2. As shown in Figure 5 (right) and Table 2, it can be expected for pNPA having a smallest oxidation potential and the highest HOMO energy level among copolymers due to its built-in electron-rich moiety (naphthylphenylamine). Similarly, pCBZ has a second small oxidation potential and the second high HOMO energy level next to that of pNPA. This is because the *N*-carbazole moiety is less electron-rich than that of naphthylphenylamine. On the other hand, it is reasonable to find pOXD with the highest oxidation potential and the lowest HOMO energy level among copolymers due to its built-in electron-deficient moiety (oxadiazole heterocyclic ring). By calculating the optical band gaps (from the on-set absorption energy of thin film) and HOMO energy levels (obtained from AC-2 or DPV), the LUMO energy level of each copolymer can be obtained, and they are summarized in Table 2. For a similar reason (built-in electron-deficient moiety), the deepest LUMO energy level was found for pOXD among these copolymers.

Hole-Blocking/Electron-Transporting and Cathode Configuration of PLEDs. The initial examinations of electroluminescent properties for these copolymers were conducted by fabricating multilayer devices with the configuration of ITO/PEDOT:PSS/PVK/copolymers/cathodes, where PEDOT:PSS and PVK were used as hole injection and hole transporting layers, respectively. Four different cathode configurations, TPBI/LiF/Al, CsF/Ca/Al, TPBI/CsF/Al, and CsF/Al, were tested to investigate the cathode effect on the electroluminescence of PLEDs. TPBI (2,2',2''-(1,3,5-phenylene)-tris-(1-phenyl-1*H*-benzimidazole) was used as the hole-blocking/electron-transporting layer after the polymer light-emitting

layer. A thin layer of LiF or CsF was used as the electron-injection layer followed by Ca and/or Al as the cathode material. Figure 6 showed the EL characteristics based on copolymer pOXD with four different cathode configurations with or without TPBI.

It is apparent that devices incorporated with TPBI show higher luminous efficiencies than those without TPBI. It is also clear that the device taking Ca as the cathode shows a slightly higher EL efficiency than that without Ca. We presume a better charge balance between electron and hole in these devices (ones with TPBI and/or Ca). And this may be attributed to the blocking of hole carriers and the enhancement of the electron-injection because of TPBI or the low work function Ca as the cathode material. However, an emission shoulder was observed around 500 nm in the green portion of EL spectra, whenever the devices were incorporated with either TPBI as the hole-blocking/electron-transporting layer or the low work function Ca as the cathode material. Such enhanced-green EL has been reported before, and it can be attributed to the optical microcavity effect,²⁰ which improves light out coupling in the green portion of the EL spectrum. We have observed a similar effect taking place on other anthrylene copolymers such as pDPV and pCBZ. Nevertheless, more electrons are able to penetrate into the active layer (with the aid of electron-transporting TPBI or low work function Ca), and the exciton profile (light-emitting zone) within the active layer may be shifted away from the cathode. This significantly reduced exciton quenching adjacent to cathode surface, and thus EL efficiency is enhanced.

OXD-7-Doped PLEDs. Similar enhancement of the green portion of EL spectra has been reported before on a solution-processed blue electrophosphorescent OLEDs doped with electron-transporting OXD-7 (1,3-bis(2-(4-*tert*-butylphenyl)-1,3,4-oxadiazol-5-yl)benzene).^{20c,d} Such enhancement was also observed in our copolymer PLEDs when doped with OXD-7. Here, we adopted the device configuration of

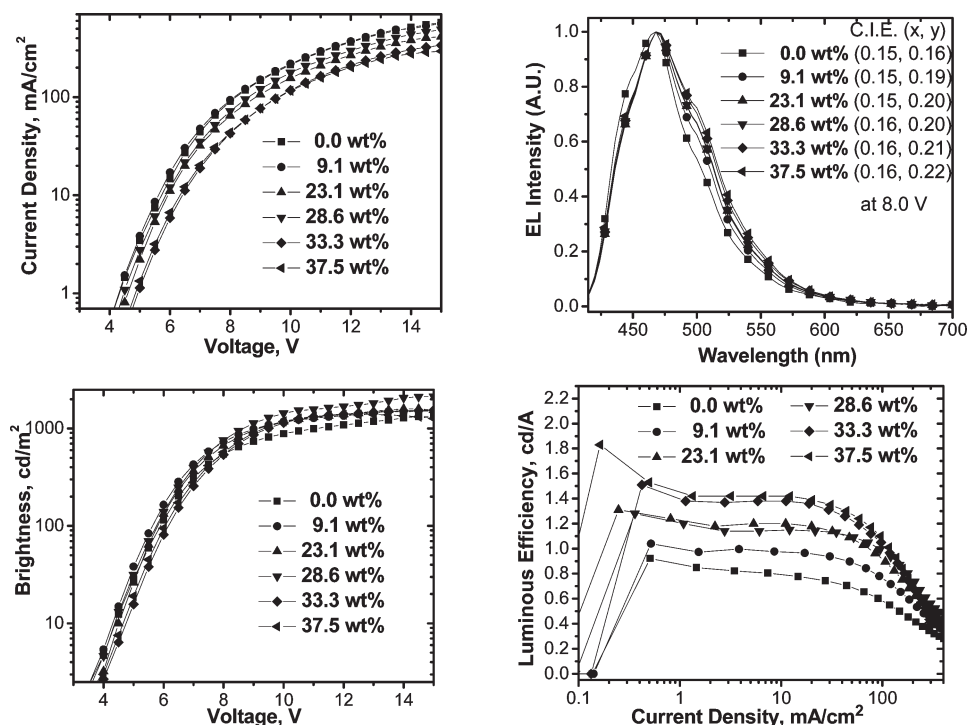


Figure 7. Electroluminescence (EL) characteristics of OXD-7-doped PLED devices with the device configuration of ITO/PEDOT:PSS/PVK/pOXD:OXD-7 (x wt %, $x = 0.0, 9.1, 23.1, 28.6, 33.3, 37.5$)/CsF(1 nm)/Al(120 nm).

Table 3. Electroluminescence Characteristics of PLEDs Containing 2,6-Linked Anthrylenophenylene Copolymers^a

	turn-on voltage ^b (V)	EL brightness max, 100 mA/cm ² , 10 mA/cm ² (cd/m ²)	luminous efficiency at 10 and 100 mA/cm ² (cd/A)	Δ_{LE}^c (cd/A)	max efficiency (cd/A, lm/W)	λ_{max}^{EL} , fwhm (nm) at 8 V	1931 CIE chromaticity (x, y) at 8.0 V
pDPA	3.8	2430, 1053, 119	1.17, 1.05	0.12	1.26, 0.53	469, 103	0.19, 0.30
pDPV	3.7	2810, 1899, 211	2.10, 1.89	0.21	2.21, 1.01	473, 72	0.16, 0.28
pCBZ	3.2	1640, 1079, 210	2.12, 1.07	1.05	2.15, 1.02	469, 73	0.15, 0.22
pOXD	3.3	3920, 1558, 169	1.68, 1.55	0.13	1.77, 0.98	468, 85	0.17, 0.25
pTPS	4.2	264, 201, 49	0.50, 0.20	0.3	0.70, 0.40	463, 99	0.18, 0.23
pNPA	3.2	898, 611, 133	1.36, 0.60	0.76	1.36, 0.63	469, 82	0.16, 0.24

^aDevice configuration: ITO/PEDOT:PSS(40–50 nm)/PVK(20–30 nm)/copolymers (80 nm)/TPBI (25 nm)/LiF(1.0 nm)/Al(120 nm). ^bWith electroluminescence at 1 cd/m. ^cThe luminous efficiency difference between current density of 10 and 100 mA/cm².

ITO/PEDOT:PSS/PVK/pOXD:OXD-7 (x wt %, $x = 0, 9.1, 23.1, 28.6, 33.3, 37.5$)/CsF/Al to eliminate the electronic effect from TPBI and Ca. The EL results of these OXD-7 doped PLEDs are displayed in Figure 7.

As shown in Figure 7, the EL spectrum of the nondoped PLED device (0 wt %) exhibits a pure blue-light emission with CIE coordinates (0.15, 0.16). However, the emission shoulder around 500 nm enlarged when the doping concentration of OXD-7 in the polymer layer increased. Introducing OXD-7 into the polymer layer as an electron-transporting moiety also resulted a pronounced enhancement of PLED brightness and luminous efficiency. Similar to that shown in the previous section, the enhanced luminous efficiency may be attributed to a better charge balance between electrons and holes through the enhancement of electron transport by OXD-7 dopant. On the basis of the above tests, it is inferable that these diphenylanthracene-based blue PLEDs are abundant in hole carriers, even though the tested copolymer pOXD is relatively electron-deficient (electron transporting) among the series.

2,6-Linked Anthrylenophenylene Copolymer PLEDs. Having above examinations, we chose the most favorable device configuration, ITO/PEDOT:PSS/PVK/copolymer/TPBI/LiF/Al, to investigate EL characteristics of all copolymers, and the results are summarized in Table 3 and Figure 8.

These PLEDs emitted blue to sky-blue EL with main emission band peaked around 463–473 nm, corresponding to CIE coordinates of (0.15, 0.22) to (0.19, 0.30). The EL spectrum of the nonsubstituted polymer pDPA has an emission shoulder around 500 nm with fwhm (full width at half-maximum) of 103 nm, which is significantly broader than the other copolymers. This may be ascribed to the lack of bulky substituent of pDPA resulting polymer chain aggregation. Whereas pDPV PLED exhibited the highest luminous efficiency of 2.21 cd/A among all copolymers, pTPS PLED showed a low efficiency of 0.70 cd/A with maximum luminance of only 264 cd/m². The poor PLED performance of pTPS can be attributed to its low molecular weight and the poor film morphology in spite of its high solid-state fluorescence quantum yields compared with other copolymers, although poor charge-transporting properties of pTPS due to the nonplanar and bulky triphenylsilyl group could be an alternative reason.

Interestingly, we have found that the PLEDs with the lowest turn-on voltage (3.2 or 3.3 V) belong to three charge-transporting copolymers (see turn-on voltage data in Table 3). They are pOXD for electron-transporting and pCBZ and pNPA for hole-transporting, and all their PLED efficiencies are superior to the unsubstituted pDPA. The enhanced PLED efficiency can be ascribed to the reinforcement of

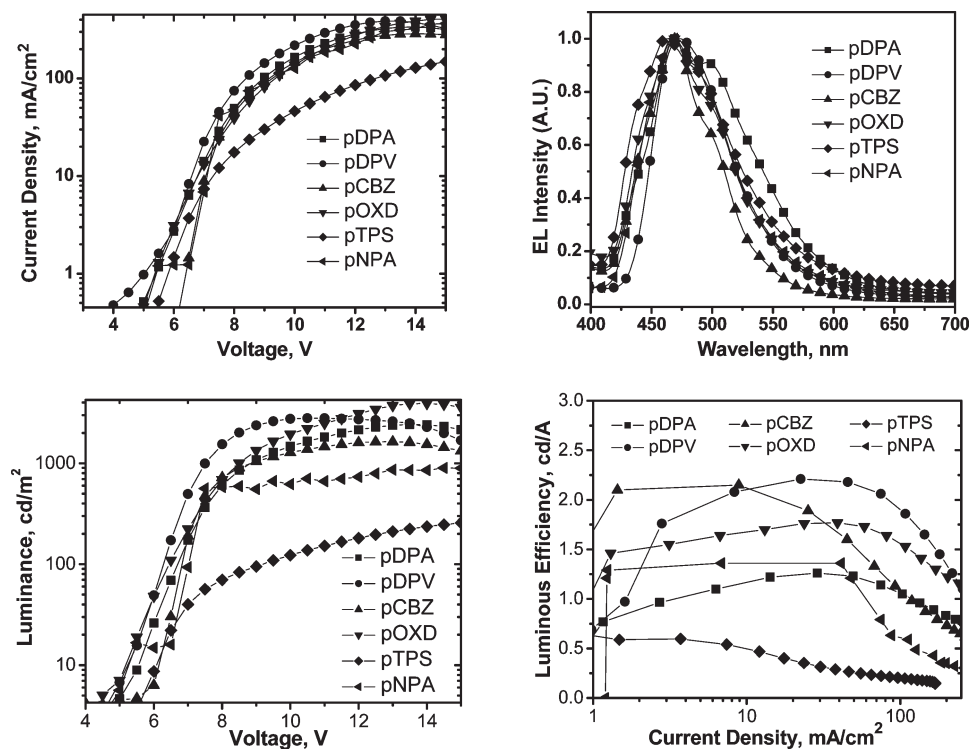


Figure 8. Electroluminescence (EL) characteristics of copolymers based on the device configuration of ITO/PEDOT:PSS(50 nm)/PVK(20 nm)/copolymers(80 nm)/TPBI(25 nm)/LiF(1 nm)/Al(120 nm).

the electron- or hole-transporting abilities of 9,10-diphenylanthracene derivatives. Such charge-transporting molecular design has been applied on 9,10-diphenylanthracene-based small molecule OLEDs before.^{4a,d,e} In addition to the hole-transporting characteristics, pCBZ PLED showed the blue EL ($\text{CIE}_{x,y} = 0.15, 0.22$) with the highest blue color purity among all copolymers. Although the maximum luminous efficiency of pCBZ PLED (2.15 cd/A) is not the best, next to 2.21 cd/A of sky-blue pDPV PLED, we consider pCBZ is the best blue-light-emitting copolymer regarding the blue color purity. This can be ascribed to its relatively high solid-state fluorescence quantum yield ($\Phi_f = 37\%$) and its bulky substituent, which prevents the copolymer chain from aggregation and hence red-shifting emission wavelength.

The difference between hole- and electron-transport shows in EL efficiency roll-off. In a range of the current density between 10 and 100 mA/cm^2 , the luminous efficiency of pCBZ PLED has a significant decay ($\Delta_{\text{LE}} = 1.05 \text{ cd}/\text{A}$). Such efficiency roll-off was also observed for another hole-transporting copolymer pNPA ($\Delta_{\text{LE}} = 0.76 \text{ cd}/\text{A}$). In contrast, electron-transporting pOXD PLED showed minor efficiency roll-off, only 0.13 cd/A of Δ_{LE} (Table 3 and Figure 8). This result demonstrates that a better balance of charge transport can be achieved under high current densities when an electron-transporting moiety is incorporated into the 9,10-diphenylanthracene-based copolymers. Such reasoning is also consistent with the observed result of OXD-7 doped PLEDs, which exhibit enhanced luminous efficiency with increasing OXD-7 dopant concentrations.

According to the above examinations, we can conclude that the EL efficiency and the color purity of these 9,10-diphenylanthracene-based PLEDs are mainly affected by the balance of charge transport and the interpolymer chain aggregations. With appropriate chemical structure substituent on 9,10-diphenylanthracene, the red-shifting of EL is largely inhibited and the EL efficiency is substantially improved. Compared with other 9,10-diphenylanthracene-based light-emitting

polymers,^{6–9} which have the EL brightness less than 1000 cd/m^2 and luminous efficiency rarely over 1 cd/A , our judiciously designed copolymers have outperformed the others in PLED applications.

Conclusion

In this paper, we have successfully designed and synthesized a series of novel 2,6-linked 9,10-diphenylanthracene-based blue-light-emitting copolymers. These copolymers are composed of anthrylene and phenylene as the polymer backbone unit and a range of functional side groups appended to the 9- and 10-positions of anthracene core. Both electron-transporting and hole-transporting as well as bulky substituent as side groups of the polymer chain were studied for their thermal, electrochemical, photophysical, and electroluminescent properties. Fundamentally, we have demonstrated that both hole- and electron-transporting substituents apparently enhance the EL performance (EL color purity and efficiency) of these 2,6-anthrylenephenylene blue-light-emitting copolymers. A better hole/electron charge balance is presumably achieved in the electron-transport substituted copolymer. Our results successfully demonstrate a rational design of polyanthrylenephenylene for blue PLEDs applications.

Acknowledgment. This research was supported by the National Science Council of Taiwan, Taiwan International Graduate Program of Academia Sinica, and National Taiwan University.

References and Notes

- (1) (a) Kim, D. Y.; Cho, H. N.; Kim, C. Y. *Prog. Polym. Sci.* **2000**, *25*, 1089. (b) Bernius, M. T.; Inbasekaran, M.; O'Brien, J.; Wu, W. *Adv. Mater.* **2000**, *12*, 1737. (c) Chen, S.-A.; Lu, H.-H.; Huang, C.-W. *Adv. Polym. Sci.* **2008**, *212*, 49. (d) Grimsdale, A. C.; Chan, K. L.; Martin, R. E.; Jokisz, P. G.; Holmes, A. B. *Chem. Rev.* **2009**, *109*, 897.
- (2) Chan, K. L.; McKiernan, M. J.; Towns, C. R.; Holmes, A. B. *J. Am. Chem. Soc.* **2005**, *127*, 7662.
- (3) Pope, M.; Kallmann, H. P.; Magnante, P. *J. Chem. Phys.* **1963**, *38*, 2042.

- (4) (a) Danel, K.; Huang, T.-H.; Lin, J. T.; Tao, Y.-T.; Chuen, C.-H. *Chem. Mater.* **2002**, *14*, 3860. (b) Kim, Y. H.; Jeong, H. C.; Kim, S. H.; Yang, K.; Kwon, S. K. *Adv. Funct. Mater.* **2005**, *15*, 1799. (c) Lee, T.; Song, K. H.; Jung, I.; Kang, Y.; Lee, S. H.; Kang, S. O.; Ko, J. *J. Organomet. Chem.* **2006**, *691*, 1887. (d) Chien, C.-H.; Chen, C.-K.; Hsu, F.-M.; Shu, C.-F.; Chou, P.-T.; Lai, C.-H. *Adv. Funct. Mater.* **2009**, *19*, 560. (e) Wu, C.-H.; Chien, C.-H.; Hsu, F.-M.; Shih, P.-I.; Shu, C.-F. *J. Mater. Chem.* **2009**, *19*, 1464.
- (5) (a) Jiang, X. Y.; Zhang, Z. L.; Zheng, X. Y.; Wu, Y. Z.; Xu, S. H. *Thin Solid Films* **2001**, *401*, 251. (b) Shi, J.; Tang, C. W. *Appl. Phys. Lett.* **2002**, *80*, 3201. (c) Zhang, X. H.; Liu, M. W.; Wong, O. Y.; Lee, C. S.; Kwong, H. L.; Lee, S. T.; Wu, S. K. *Chem. Phys. Lett.* **2003**, *369*, 478. (d) Lee, M.-T.; Chen, H.-H.; Liao, C.-H.; Tsai, C.-H.; Chen, C. H. *Appl. Phys. Lett.* **2004**, *85*, 3301.
- (6) (a) Satoh, S.; Suzuki, H.; Kimata, Y.; Kuriyama, A. *Synth. Met.* **1996**, *79*, 97. (b) Kim, Y.; Kwon, S.; Yoo, D.; Rubner, M. F.; Wrighton, M. S. *Chem. Mater.* **1997**, *9*, 2699. (c) Hirohata, M.; Tada, K.; Kawai, T.; Onoda, M.; Yoshino, K. *Synth. Met.* **1997**, *85*, 1273. (d) Klärner, G.; Davey, M. H.; Chen, W. D.; Scott, J. C.; Miller, R. D. *Adv. Mater.* **1998**, *10*, 993. (e) Mal'tsev, E. I.; Brusentseva, M. A.; Lypenko, D. A.; Berendyaev, V. I.; Kolesnikov, V. A.; Kotov, B. V.; Vannikov, A. V. *Polym. Adv. Technol.* **2000**, *11*, 325. (f) Park, L. S.; Han, Y. S.; Hwang, J. S.; Kim, S. D. *J. Polym. Sci., Part A: Polym. Chem.* **2000**, *38*, 3173. (g) Marsitzky, D.; Scott, J. C.; Chen, J. P.; Lee, V. Y.; Miller, R. D.; Setayesh, S.; Müllen, K. *Adv. Mater.* **2001**, *13*, 1096. (h) Zheng, S.; Shi, J. *Chem. Mater.* **2001**, *13*, 4405. (i) Kim, Y. H.; Bark, K. M.; Kwon, S. K. *Bull. Korean Chem. Soc.* **2001**, *22*, 975. (j) Huang, J.; Niu, Y.; Xu, Y.; Hou, Q.; Yang, W.; Mo, Y.; Yuan, M.; Cao, Y. *Synth. Met.* **2003**, *135*, 181. (k) Ha, J.; Vacha, M.; Khanchaitit, P.; Ath-Ong, D.; Lee, S. H.; Ogino, K.; Sato, H. *Synth. Met.* **2004**, *144*, 151. (l) Kim, Y. H.; Kwon, S. K. *J. Appl. Polym. Sci.* **2006**, *100*, 2151. (m) Ohshita, J.; Kangai, S.; Tada, Y.; Yoshida, H.; Sakamaki, K.; Kunai, A.; Kunugi, Y. *J. Organomet. Chem.* **2007**, *692*, 1020. (n) Sun, J.; Cheng, J. G.; Zhu, W. Q.; Ren, S. J.; Zhong, H. L.; Zeng, D. L.; Du, J. P.; Xu, E. J.; Liu, Y. C.; Fang, Q. *J. Polym. Sci., Part A: Polym. Chem.* **2008**, *46*, 5616.
- (o) Mo, Y. Q.; Deng, X. Y.; Jiang, X.; Cui, Q. H. *J. Polym. Sci., Part A: Polym. Chem.* **2009**, *47*, 3286.
- (7) (a) Boyd, T. J.; Geerts, Y.; Lee, J. K.; Fogg, D. E.; Lavoie, G. G.; Schrock, R. R.; Rubner, M. F. *Macromolecules* **1997**, *30*, 3553. (b) Boyd, T. J.; Schrock, R. R. *Macromolecules* **1999**, *32*, 6608.
- (8) Sun, J.; Chen, J.; Zou, J.; Ren, S.; Zhong, H.; Zeng, D.; Du, J.; Xu, E.; Fang, Q. *Polymer* **2008**, *49*, 2282.
- (9) Chung, S. J.; Jin, J. I.; Lee, C. H.; Lee, C. E. *Adv. Mater.* **1998**, *10*, 684.
- (10) de Mello, J.; Wittmann, H.; Friend, R. *Adv. Mater.* **1997**, *9*, 230.
- (11) Rehahn, M.; Schlüter, A.-D.; Feast, W. J. *Synthesis* **1988**, *5*, 386–388.
- (12) Chanteau, S.; Tour, J. *J. Org. Chem.* **2003**, *68*, 8750.
- (13) Wang, Y.; Hou, Z. *J. Am. Chem. Soc.* **2006**, *128*, 17.
- (14) Ito, K.; Suzuki, T.; Sakamoto, Y.; Kubota, D.; Inoue, Y.; Sato, F.; Tokito, S. *Angew. Chem., Int. Ed.* **2003**, *42*, 1159.
- (15) Wang, S.; Oldham, J. W.; Hudack, J. R.; Bazan, G. J. *Am. Chem. Soc.* **2000**, *122*, 5695.
- (16) (a) Cui, W.; Wu, Y.; Tian, H.; Geng, Y.; Wang, F. *Chem. Commun.* **2008**, 1017. (b) Sun, J.; Chen, J.; Zou, J.; Ren, S.; Zhong, H.; Zeng, D.; Du, J.; Xu, E.; Fang, Q. *Polymer* **2008**, *49*, 2282. (c) Jo, W. J.; Kim, K. H.; No, H. C.; Shin, D. Y.; Oh, S. J.; Son, J. H.; Kim, Y. H.; Cho, Y. K.; Zhao, Q. H.; Lee, K. H.; Oh, H. Y.; Kwon, S. K. *Synth. Met.* **2009**, *159*, 1359.
- (17) (a) Cui, W.; Zhang, X.; Jiang, X.; Tian, H.; Yan, D.; Geng, Y.; Jing, X.; Wang, F. *Org. Lett.* **2006**, *8*, 785. (b) Cui, W.; Zhao, Y.; Tian, H.; Xie, Z.; Geng, Y.; Wang, F. *Macromolecules* **2009**, *42*, 8021.
- (18) Berlman, I. B., Ed. *Handbook of Fluorescence Spectra of Aromatic Molecules*, 2nd ed.; Academic Press: New York, 1971.
- (19) Chiang, C.-L.; Tseng, S.-M.; Chen, C.-T.; Hsu, C.-P.; Shu, C.-F. *Adv. Funct. Mater.* **2008**, *18*, 248.
- (20) (a) Nakamura, T.; Tsutsumi, N. *J. Appl. Phys.* **2004**, *96*, 6016. (b) Wu, Z.; Wang, L.; Lei, G.; Qiu, Y. *J. Appl. Phys.* **2005**, *97*, 103105. (c) Krummacker, B.; Mathai, M. K.; Choong, V. E.; Choulis, S. A.; So, F.; Winnacker, A. *Org. Electron.* **2006**, *7*, 313. (d) Mathai, M. K.; Choong, V. E.; Choulis, S. A.; Krummacker, B.; So, F. *Appl. Phys. Lett.* **2006**, *88*, 243512.